

Photonic bandgap engineering with inverse opal multistacks of different refractive index contrasts

Dae-Kue Hwang,¹ Heeso Noh,² Hui Cao,² and Robert P. H. Chang^{1,a)}

¹Materials Research Institute, Northwestern University, Evanston, Illinois 60208, USA

²Department of Applied Physics, Yale University, New Haven, Connecticut 06520, USA

(Received 27 May 2009; accepted 11 August 2009; published online 31 August 2009)

We have self-assembled photonic crystal with a multistack structure using same size of spheres but from materials with different refractive indices. Al₂O₃, ZnO, and TiO₂ are infiltrated into opal templates by atomic layer deposition. Stacking multiple inverse opal structures with different refractive index contrasts broadens the reflection bands dramatically. Numerical simulations with plane wave expansion method show good agreement with experimental results. © 2009 American Institute of Physics. [DOI: 10.1063/1.3216582]

Photonic crystals (PCs) are dielectric materials artificially structured on an optical length scale. The periodic modulation of the refractive index introduces stop bands (or gaps) in the optical band structure. When photonic bandgap (PBG) materials are formed, they provide unique optical properties that are the basis for numerous applications.^{1–7} Various fabrication methods have been proposed to meet the technological challenge of forming PBG.^{8–13} Self-assembled colloidal crystals,^{14–16} which are collectively called artificial opals, are the most widely studied three-dimensional (3D) PCs to date. Owing to a relatively straightforward and cost-effective preparation technique, opals are often considered as a benchmark for 3D PCs prepared by other methods. The quality of the artificial structure, which will be related to as crystal quality, is the most important parameter in determining the performance of PCs in optical applications. We recently reported the fabrication of inverted opal ZnO PCs exhibiting strong PBGs and good luminescence.^{17,18} The inverse opal was formed using a low-temperature atomic layer deposition (ALD) technique to infiltrate ZnO between polystyrene (PS), which was subsequently removed by firing in air at 500 °C. In this letter, we report photonic band engineering of an inverse opal by creating multistack inverse opal of different refractive indices but same lattice constant to broaden the reflection bands of the PC.

The opal templates were prepared using a vertical deposition technique detailed elsewhere.¹⁹ Glass substrates were placed in vials with deionized water containing between 0.1 and 0.3 vol % PS spheres in suspension, depending on sphere size and intended opal film thickness. The water was then slowly evaporated at 50 °C in a drying oven. This method yields PS opal films with controllable thicknesses between 20 and 100 layers and large single crystalline domains, oriented with the (111) planes of the face-centered-cubic (fcc) structure parallel to the substrate surface. Al₂O₃, ZnO, and TiO₂ were infiltrated into the opal templates by ALD (Ref. 20) using trimethylaluminum (TMA), diethyl zinc (DEtZn), and titaniumtetrachloride (TiCl₄), respectively, and water (H₂O) as precursors. To avoid deformation or melting of the PS structures, the growth temperature was kept at 85 °C, below the glass transition temperature of PS. The chamber pressure during growth was kept at 10 Torr and

a relatively slow flow of N₂ carrier gas was maintained in the chamber. One ALD reaction cycle consisted of a 1 s exposure to TMA, DEtZn, or TiCl₄ followed by a 20 s N₂ purge, and a 1 s exposure to H₂O vapor, followed another 20 s N₂ purge. Each exposure sequence resulted in the growth of a partial monolayer of Al₂O₃, ZnO, and TiO₂, with a corresponding growth rate of 0.15, 0.2, and 0.17 nm per cycle on a flat surface. The ALD reaction cycle was optimized for efficient diffusion of precursors into and full infiltration of the opal templates and while minimizing the formation of excess oxide layer on the outer surface of the template. Once the open porosity of the opal is closed off, an excess layer of Al₂O₃, ZnO, or TiO₂ formed on the outer surfaces of the templates, indicating complete infiltration. Optical reflectivity was measured by UV/visible/near IR spectrometer (Perkin Elmer LAMBDA 1050) with wavelength range of 185–3300 nm. The sample mount had two settings for measuring diffuse (scattered) reflectivity and total (diffuse and specular) reflectivity. Specularly reflected light was tightly reflected around the angle of incidence (mirrorlike reflection). Diffusely reflected light result from roughness, defects, etc., and was collected by an integrating sphere. The inverse opals were mounted to the diffuse reflectance accessory sphere such that the [111] direction was pointing almost directly inwards. Specular reflectivity spectra were taken by subtracting the diffuse reflectivity from the total reflectivity. We calculated photonic band structure using the plane wave expansion method (MIT Photonic-Bands package) developed by Steven G. Johnson at MIT along with the Joannopoulos *ab initio* Physics group.

Figure 1 shows the schematic illustration of the sample preparation. For these studies, we prepared two kinds of multistack samples: Al₂O₃/TiO₂ and Al₂O₃/ZnO/TiO₂. The PS opal template of sphere size 270 nm was prepared using a vertical deposition technique, Fig. 1(a). The opal template was infiltrated by ALD using 90 cycles of TiCl₄ and H₂O, Fig. 1(b). A second opal template with same size of sphere as opal for the TiO₂ layer was prepared on the TiO₂ infiltrated template using a vertical deposition technique, Fig. 1(c), and then ZnO is infiltrated into the template by ALD using 80 cycles of DEtZn and H₂O, Fig. 1(d). A third template for infiltration of Al₂O₃ was prepared on top of the multilayer ZnO and TiO₂ infiltrated templates, Fig. 1(e), and then infiltrated using 100 cycles of TMA and H₂O, Fig. 1(f). The PS

^{a)}Electronic mail: r-chang@northwestern.edu.

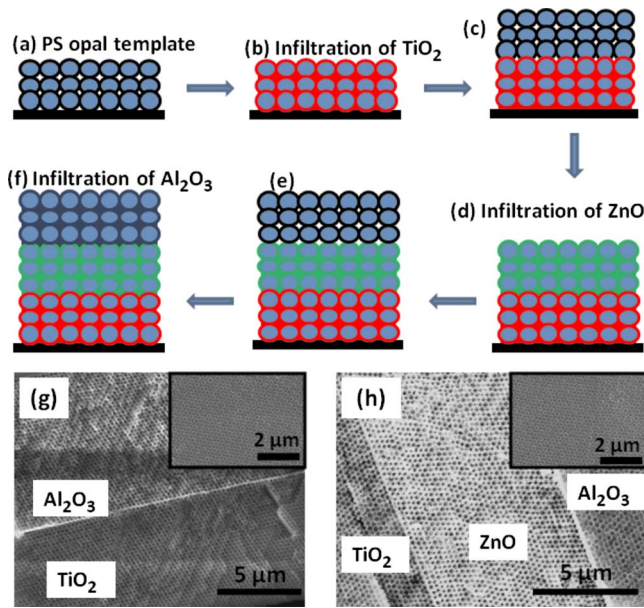


FIG. 1. (Color online) Schematic illustration for fabrication of multistack opal structure using different index materials such as Al_2O_3 , ZnO and TiO_2 .

spheres were then removed by firing the structure in air at 500°C for 1 h, leaving an ordered fcc array of air holes in the $\text{Al}_2\text{O}_3/\text{ZnO}/\text{TiO}_2$ multilayer. Figures 1(g) and 1(h) show the cross-sectional scanning electron microscopy (SEM) images of double multistack ($\text{Al}_2\text{O}_3/\text{TiO}_2$) and triple multistack ($\text{Al}_2\text{O}_3/\text{ZnO}/\text{TiO}_2$) inverse opal structure. The cross-sectional and inset (top view) SEM images show that the multistack inverse opal structure have abrupt interfaces and well ordered structures.

Figure 2 shows the optical reflectivity spectra for a single stack of inverse opal structure. The blue line (bottom curve) represents spectrum from an Al_2O_3 [refractive index of $n=1.7$ (Ref. 21)] inverse opal structure which shows a reflection peak at 492 nm corresponding to the lowest PBG. The green line (middle curve) represents spectrum from ZnO [refractive index of $n=2.0$ (Ref. 22)] inverse opal structure

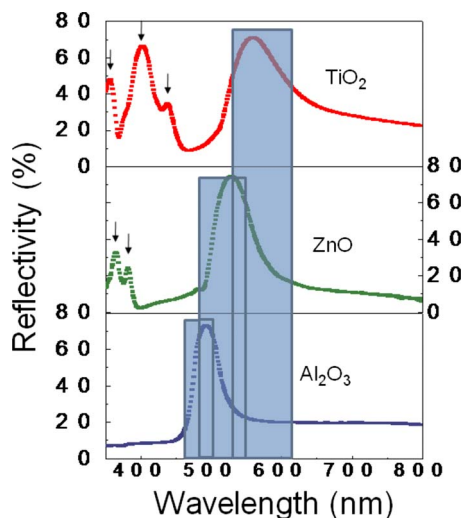


FIG. 2. (Color online) Normal-incidence reflection spectra of Al_2O_3 [blue line (bottom)], ZnO [green line (middle)] and TiO_2 [red line (top)] single-stack inverse opal structure, respectively. Measured reflection spectra of the inverse opals and calculated positions of the first gap are shown in gray shaded area.

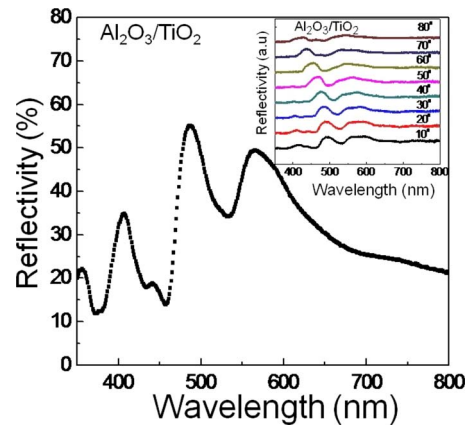


FIG. 3. (Color online) Normal and off-normal (inset)-incidence reflection spectra of $\text{Al}_2\text{O}_3/\text{TiO}_2$ double-stack inverse opal structure.

which shows the main reflection peak at 526 nm corresponding to the lowest PBG and additional reflection spectra peaks at 382 and 365 nm as marked by arrows in Fig. 2. The red line (top curve) shows the reflection spectrum of TiO_2 [refractive index of $n=2.5$ (Ref. 23)] inverse opal structure. It consists of a broad reflection peak at 564 nm corresponding to the fundamental PBG and additional reflection spectra peaks at 439, 402, and 357 nm as marked by arrows. TiO_2 has a relatively large refractive index,²³ thus we observed stronger reflection peaks from the TiO_2 inverse opal as compared to Al_2O_3 and ZnO inverse opals. The peak positions can be related to the sphere diameter and the effective refractive index of the medium using Bragg's law, $\lambda_{\text{max}} = 2n_{\text{eff}}d_{111}$, where d_{111} is the 111 lattice spacing. We can confirm that the difference in frequency of reflection peaks come from different effective refractive indices of the inverse opal structures because the same size of spheres were used in all the experiments. The single layers show reflectivity peaks amplitude around 70% at the lowest PBG.

Figure 3 shows reflection spectra of the double multistack ($\text{Al}_2\text{O}_3/\text{TiO}_2$). The peaks around 357, 407, 443, 487, and 567 nm arise from the Bragg diffraction of incident light within each stack of Al_2O_3 and TiO_2 inverse opal, as seen in Fig. 2. The spectrum shows a clear dip in reflection between wavelength 487 and 567 nm and other reflection peaks at 357, 407, and 443 nm with a low reflection compared to the single inverse opal structure of TiO_2 . In the context of PCs, the mismatch of optical modes between different stacks can be used for light localization and guiding in prospective optical devices. We note that the reflection spectra of the multistack have features which correspond to reflection peaks of individual single-stack inverse opal structures. This correspondence confirms the high crystalline quality of each stack of the composite sample, and also suggests that the optical property of the composite system is a combination of those of the individual stacks.

The theoretically predicted photonic band structure of Al_2O_3 ($n=1.7$), ZnO ($n=2.0$) and TiO_2 ($n=2.5$) inverse opal are shown in Fig. 4. To compare the optical measurement to the band structure calculations we first determined the lattice constant from SEM measurement. We obtained a fcc lattice constant of 367 nm from the 260 nm diameter inverse opal. The Al_2O_3 inverse opal has only one PBG in the Γ -L direction (111) within the frequency range of calculation. The

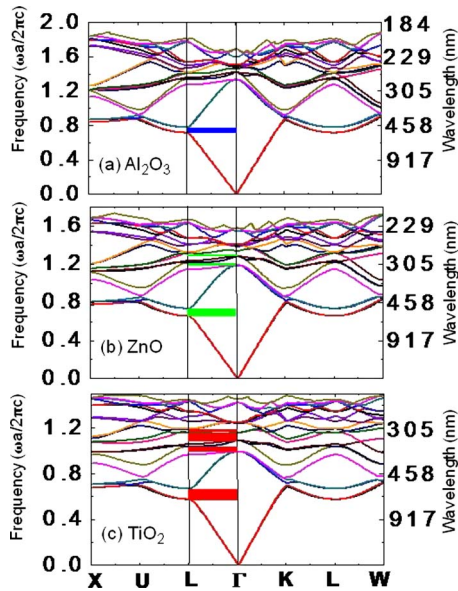


FIG. 4. (Color online) Simulated photonic band structure of (a) Al_2O_3 ($n=1.7$), (b) ZnO ($n=2.0$) and (c) TiO_2 ($n=2.5$) inverse opal in the Γ -L direction [111]. Shaded regions in (a), (b), and (c) show the calculated positions of the gaps.

wavelength of gap center is 494 nm, as shown in Fig. 4(a). The ZnO inverse opal shows three PBGs with the center of the first gap at 526 nm as shown in Fig. 4(b). The TiO_2 inverse opal shows four PBGs with the center of the first gap at 593 nm, as shown in Fig. 4(c). The above results as shown in gray shaded area in Fig. 2 give the appropriate width for the first gaps. Good agreement is also obtained with the frequency of the reflection peak in the reflection spectra and the center of the first PBG.

The reflection spectra of the three multistack ($\text{Al}_2\text{O}_3/\text{ZnO}/\text{TiO}_2$) is shown in Fig. 5. The peaks around 490, 517, and 558 nm arise from the first-order PBG of each layer in the stack of Al_2O_3 , ZnO , and TiO_2 , as seen in Fig. 2. The other reflection peaks at 387 and 407 nm show as weaker than those of single or double stacks. We assumed that the decrease of reflection intensity at short wavelength is

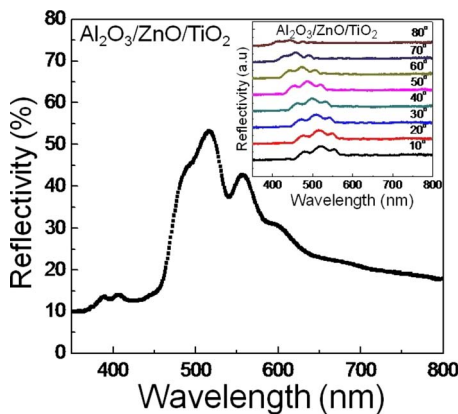


FIG. 5. (Color online) Normal and off-normal (inset)-incidence reflection spectra of $\text{Al}_2\text{O}_3/\text{ZnO}/\text{TiO}_2$ multistack inverse opal structure.

due to absorption of ZnO surface layer. The triple multistack layers show reflectivity peak amplitude around 55% at the PBG.

Angle-resolved reflectivity was used to measure the behavior of PBG of multistack inverse opal structure, as shown in the inset of Figs. 3 and 5. First-order PBG blueshifts and the bandgap narrows with increasing angle of incident.

In summary, we have fabricated multistack inverse opal with different refractive index materials. To reduce disorder in the self-assemble process of multiple opal templates, spheres of same size are used. Different index materials, such as Al_2O_3 , ZnO , and TiO_2 are infiltrated into the multistack opal templates by ALD. Optical reflection measurements show that a significant broadening of reflection bands in [111] direction. It suggests that by overlapping many inverse opal structures with the same sphere sizes but different refractive index, the effective band width can be increased and inhibit light propagation over a wider range of wavelength and, presumably, a wider angle range as well. This may be a viable strategy for creating functional optical filters or optical devices.

This research has been funded by NSF Grant No. ECCS-0823345 and the use of central facilities has been funded by NSF under Grant No. DMR-0520513.

- ¹E. Yablonovitch, *Phys. Rev. Lett.* **58**, 2059 (1987).
- ²R. D. Meade, A. Devenyi, J. D. Joannopoulos, O. L. Alerhand, D. A. Smith, and K. Kash, *J. Appl. Phys.* **75**, 4753 (1994).
- ³S. H. Fan, J. N. Winn, A. Devenyi, J. C. Chen, R. D. Meade, and J. D. Joannopoulos, *J. Opt. Soc. Am. B* **12**, 1267 (1995).
- ⁴A. Mekis, J. C. Chen, I. Kurland, S. H. Fan, P. R. Villeneuve, and J. D. Joannopoulos, *Phys. Rev. Lett.* **77**, 3787 (1996).
- ⁵J. D. Joannopoulos, P. R. Villeneuve, and S. H. Fan, *Nature (London)* **386**, 143 (1997).
- ⁶Y. Fink, J. N. Winn, S. H. Fan, C. P. Chen, J. Michel, J. D. Joannopoulos, and E. L. Thomas, *Science* **282**, 1679 (1998).
- ⁷P. Russell, *Science* **299**, 358 (2003).
- ⁸S. Y. Lin, J. G. Fleming, D. L. Hetherington, B. K. Smith, R. Biswas, K. M. Ho, M. M. Sigalas, W. Zubrzycki, S. R. Kurtz, and J. Bur, *Nature (London)* **394**, 251 (1998).
- ⁹S. Noda, K. Tomoda, N. Yamamoto, and A. Chutinan, *Science* **289**, 604 (2000).
- ¹⁰S. Kawakami, O. Hanaizumi, T. Sato, Y. Ohtera, T. Kawashima, N. Yasuda, Y. Takei, and K. Miura, *Electron. Commun. Jpn., Part 2: Electron.* **82**, 43 (1999).
- ¹¹M. Campbell, D. N. Sharp, M. T. Harrison, R. G. Denning, and A. J. Turberfield, *Nature (London)* **404**, 53 (2000).
- ¹²K. Aoki, H. T. Miyazaki, H. Hirayama, K. Inoshita, T. Baba, K. Sakoda, N. Shinya, and Y. Aoyagi, *Nature Mater.* **2**, 117 (2003).
- ¹³M. Deubel, G. Von Freymann, M. Wegener, S. Pereira, K. Busch, and C. M. Soukoulis, *Nature Mater.* **3**, 444 (2004).
- ¹⁴P. N. Pusey, W. Vanmegen, P. Bartlett, B. J. Ackerson, J. G. Rarity, and S. M. Underwood, *Phys. Rev. Lett.* **63**, 2753 (1989).
- ¹⁵A. P. Gast and Y. Monovoukas, *Nature (London)* **351**, 553 (1991).
- ¹⁶Y. N. Xia, B. Gates, Y. D. Yin, and Y. Lu, *Adv. Mater.* **12**, 693 (2000).
- ¹⁷M. Scharrer, X. Wu, A. Yamilov, H. Cao, and R. P. H. Chang, *Appl. Phys. Lett.* **86**, 151113 (2005).
- ¹⁸M. Scharrer, A. Yamilov, X. H. Wu, H. Cao, and R. P. H. Chang, *Appl. Phys. Lett.* **88**, 201103 (2006).
- ¹⁹P. Jiang, J. F. Bertone, K. S. Hwang, and V. L. Colvin, *Chem. Mater.* **11**, 2132 (1999).
- ²⁰A. W. Ott and R. P. H. Chang, *Mater. Chem. Phys.* **58**, 132 (1999).
- ²¹D. Ferri, T. Burgi, and A. Baiker, *J. Phys. C* **105**, 3187 (2001).
- ²²N. Mehan, M. Tomar, V. Gupta, and A. Mansingh, *Opt. Mater.* **27**, 241 (2004).
- ²³J. Wijnhoven and W. L. Vos, *Science* **281**, 802 (1998).